

Hyperon threshold and stellar radii

Luiz L. Lopes^{1,2,*} and Debora P. Menezes¹

¹ *Universidade Federal de Santa Catarina; C.P. 476, CEP 88.040-900, Florianópolis, SC, Brasil*

² *Centro Federal de Educação Tecnológica de Minas Gerais Campus VIII; CEP 37.022-560, Varginha - MG - Brasil*

(Dated: January 13, 2017)

In this work we show how the emergence of a new degree of freedom in the nuclear bulk not only softens the EoS but reduces the radii of stars with high central density. If an enough repulsive channel, as the strange vector ϕ meson, is added to the scheme, we are able to simulate very massive and compact stars. Indeed we are able to construct an equation of state (EoS) that predicts a $2.05 M_{\odot}$ as maximum mass and a radius of 11.51 km for the canonical $1.4M_{\odot}$ in a thermodynamical consistent way. We also link the radii of the canonical stars to a soft EoS for densities not much above the nuclear saturation point. Moreover, comparing our EoS with results obtained from heavy ion collisions, we show that the presence of a new degree of freedom allows a better agreement between theory and experiment.

PACS numbers: 24.10.Jv, 26.60.Kp

I. INTRODUCTION

The physics of cold strong interacting matter at extreme densities is still not available in terrestrial laboratories. So far, the only place believed to reach such condition is the interior of neutron stars. The observations of pulsars evolved in the last years and provided us more precise information about the macroscopic characteristic of these objects.

For instance, the observations of two hyper massive pulsars, PSR J1614-2230 [1] and PSR J0348+0432 [2], show us that the EoS of beta-equilibrium nuclear matter should be very stiff, being able to produce a two solar masses neutron star. This indicates that hadron interaction at very small distances is strongly repulsive.

On other hand, the physics of neutron stars radii also improved in this decade. Recent observations indicate that the radii of pulsars of mass around the canonical $1.4M_{\odot}$ are lower than most of the previsions found in the literature [3]. Today we know that the radius of the neutron stars are somehow related to the symmetry energy slope, L [4–7], although L cannot be the ultimate information about neutron stars radii, once the same model with the same slope, predicts neutron stars whose difference in radius reaches 1.7 km [7]. Theoretical works and astrophysical observations have strongly constrained the radius of the canonical mass in the last couple of years. For example, based on a chiral effective theory, ref. [8] constrained the radii of the canonical $1.4M_{\odot}$ neutron star to 9.7-13.9 km. To fit experimental information from neutron skins, heavy ion collisions, giant dipole resonances, and dipole polarizabilities, ref. [9] constrained the neutron star radius of a canonical mass in the narrow window $10.7 \text{ km} < R < 13.1 \text{ km}$ (90% confidence). Using time-resolved spectroscopy of thermonuclear X-ray bursts observed from an object called SAX J1748.9-2021

ref. [10] constrained the radius as $R = 10.93 \pm 2.09 \text{ km}$ for a mass $M = 1.33 \pm 0.33 M_{\odot}$. From Fig. 4 of ref. [11] and Tab. 8 of ref. [12] a limit of 12.45 km is found for a neutron star of mass $1.4M_{\odot}$.

In this work we show that the onset of a new degree of freedom, not only causes the known softening of the EoS but also reduces the radii of the stars whose central density is higher than the density of the hyperon threshold (what we call here subsequent stars), when compared with the EoS without this new degree of freedom. We use here the Λ hyperon as this new degree of freedom, once it is the lowest mass baryon beyond the nucleons. Nevertheless it is important to bear in mind that the nature of the new degree of freedom is not relevant. Similar results can be obtained using Σ or Ξ hyperons, or even Δ resonances, by adjusting the strength of the coupling constant for those particles. Even more exotic particles, as dark matter [13–16] can be used without significantly affect the results.

We show that if the hyperon onset happens at relatively low density, and a channel, repulsive enough, as the strange vector ϕ meson is added, we can produce very massive and compact neutron stars in agreement with the works above mentioned. Moreover, if an attractive channel, as the strange scalar σ^* meson is also added, we can produce even more compact neutron stars. Indeed, we are able to simulate an EoS that predicts $2.05 M_{\odot}$ as maximum mass with a radius of 11.51 km for the canonical $1.4M_{\odot}$.

We also compare our results with experiences of heavy-ion collisions (HIC). In ref. [17], the authors determine the pressure of the symmetric nuclear matter up to five times nuclear saturation density. They neither exclude the onset of hyperons nor of more exotic behaviour, as the quark-hadron phase transition. We show that the emergence of a new degree of freedom also allows a better agreement of theory with experience.

This paper is organized as follows: in section II we discuss the QHD formalism and present the parametrization of the model alongside some of the physical quantities

* llopes@varginha.cefetmg.br

they foresee for nuclear matter. In section III we expose the results of the threshold of Λ hyperon in the bulk of beta-equilibrium nuclear matter and symmetric nuclear matter within four different approaches. The conclusions are drawn in section IV.

II. FORMALISM

The theory of the strong interacting matter is the QCD, where quarks interact with each other via the ex-

change of massless gauge bosons called gluons. Since the QCD has no results for dense cold matter, an effective model is required. In this work we use an extended version of the relativistic QHD [18], whose Lagrangian density reads:

$$\begin{aligned} \mathcal{L}_{QHD} = & \sum_B \bar{\psi}_B [\gamma^\mu (i\partial_\mu - g_{B\omega}\omega_\mu - g_{B\rho}\frac{1}{2}\vec{\tau} \cdot \vec{\rho}_\mu) - (m_B - g_{B\sigma}\sigma)] \psi_B - U(\sigma) + \\ & + \frac{1}{2}(\partial_\mu\sigma\partial^\mu\sigma - m_s^2\sigma^2) - \frac{1}{4}\Omega^{\mu\nu}\Omega_{\mu\nu} + \frac{1}{2}m_v^2\omega_\mu\omega^\mu + \frac{1}{2}m_\rho^2\vec{\rho}_\mu \cdot \vec{\rho}^\mu - \frac{1}{4}\mathbf{P}^{\mu\nu} \cdot \mathbf{P}_{\mu\nu}, \end{aligned} \quad (1)$$

in natural units. ψ_B are the baryonic Dirac fields, which can be the nucleons, or a new degree of freedom, in this case, Λ hyperon. The σ , ω_μ and $\vec{\rho}_\mu$ are the mesonic fields. The g 's are the Yukawa coupling constants that simulate the strong interaction, m_B is the mass of the baryon B and m_s , m_v , and m_ρ are the masses of the σ , ω , and ρ mesons respectively. The antisymmetric mesonic field strength tensors are given by their usual expressions as presented in [19]. The $U(\sigma)$ is the self-interaction term introduced in ref. [20] to reproduce some of the saturation properties of the nuclear matter and is given by:

$$U(\sigma) = \frac{1}{3!}\kappa\sigma^3 + \frac{1}{4!}\lambda\sigma^4. \quad (2)$$

Finally, $\vec{\tau}$ are the Pauli matrices. In order to describe a neutral, chemically stable matter, we add leptons as free Fermi gases:

$$\mathcal{L}_{lep} = \sum_l \bar{\psi}_l [i\gamma^\mu\partial_\mu - m_l] \psi_l, \quad (3)$$

where the sum runs over the two lightest leptons (e and μ).

The mesonic fields are obtained via mean field approximation (MFA) [18, 19, 21] and the EoS by thermodynamic relations [19, 22].

To describe the properties of nuclear matter we use a slightly modified version of the well-known GM1 parametrization [23], a widely accepted parametrization [7, 19, 21, 24–29] that is able to reasonably describe both, nuclear matter and stellar structure, consistent with experimental and astrophysical observations [28]. In this work we just reduce the strength of the ρ coupling, reducing the symmetry energy slope L from 94 MeV to 87.9 MeV [7], a value closer to what is inferred in recent observations [9, 11, 12]. This slope can be reduced even

further, [4, 30], but for the purpose of the present work, the modifications introduced in [7] suffice.

In Table I we show the parameters of the model and its previsions for five nuclear matter properties at saturation density: saturation density point (n_0), incompressibility (K), binding energy per baryon (B/A), symmetry energy (S_0) and its slope (L).

Parameters		Previsions at n_0	
$(g_{N\omega}/m_v)^2$	7.148 fm^2	n_0 (fm^{-3})	0.153
$(g_{N\sigma}/m_s)^2$	11.785 fm^2	K (MeV)	300
$(g_{N\rho}/m_\rho)^2$	3.880 fm^2	B/A (MeV)	-16.3
κ/M_N	0.005894	S_0 (MeV)	30.5
λ	-0.006426	L (MeV)	87.9

TABLE I. Slightly modified GM1 parametrization. Parameters of the model and previsions.

III. RESULTS

To study the effects of the onset of a new degree of freedom in detail, we divide this section in four different approaches. We consider the Λ hyperon only because the presence of other strange particles would make this study strongly model and parameter dependent.

A. Role of the coupling constant

The basic constituents of neutron stars are neutrons and protons in β -equilibrium. Since both are fermions, as the baryon density increases, so do the Fermi momentum and the Fermi energy, according to the Pauli principle. Ultimately, the Fermi energy exceeds the masses of the heavier baryons. The influence of the hyperons in

the EoS and neutron star mass-radius relation, strongly depend of the coupling constant of the hyperons with the mesonic field. It is well known that the Λ potential depth $U_\Lambda = -28$ MeV [23], so the coupling constants for ω and σ meson cannot be varied independently in principle. So, in this section we fix the potential depth and vary the values of the coupling constants and see how they affect the hyperon onset and population, the EoS, and consequently the mass-radius relation of the neutron stars. Similar works are found in the literature [19, 23], however, they just analyze the effects on the maximum mass. Let's study, in more detail, the influence on the radii of the neutron stars as well. In Tab. II we show four sets of values for the coupling constants utilized in this section and in Fig. 1 we plot the Λ fraction $Y_\Lambda = n_\Lambda/n$ for the four sets.

Set	$g_{\Lambda,\omega}/g_{N,\omega}$	$g_{\Lambda,\sigma}/g_{N,\sigma}$	U_Λ (MeV)
A	0.25	0.291	-28
B	0.50	0.483	-28
C	0.75	0.675	-28
D	1.00	0.865	-28

TABLE II. Different sets for Λ -mesons coupling constants with a fixed potential depth $U_\Lambda = -28$ MeV.

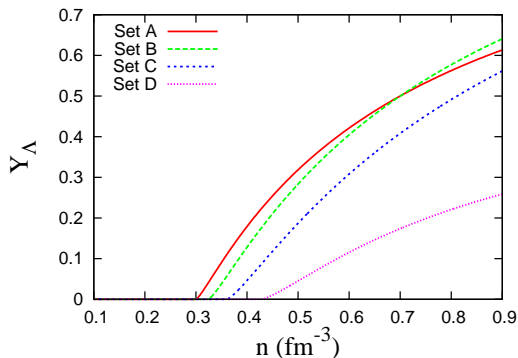


FIG. 1. (Color online) Λ threshold and population for a fixed potential depth $U_\Lambda = -28$ MeV.

We see that the higher the value of $g_{\Lambda,\omega}$, the higher the density of the hyperon threshold, varying from 0.302 fm^{-3} for set A to 0.431 fm^{-3} , for set D, ie, around 1.97 and 2.82 times the nuclear saturation density. Moreover, in general, the Λ population also increases with the increase of $g_{\Lambda,\omega}$. We can see that the curves of sets A and B cross each other (set A and C cross as well at a density around 1.2 fm^{-3}). This is due to the Pauli blocking of the hyperons in set A. Once there are more hyperons in set A at low densities, the onset of new Λ particles is more energetically favorable in set B because the Fermi sea for low Fermi moment in set A is already filled. We can also see that in set D $g_{\Lambda,\omega}$ is so high that Λ is very suppressed, Y_Λ never reaching more than 0.3, while in other sets this value could reach more than 0.6.

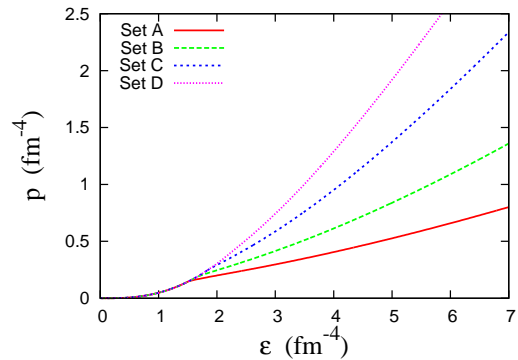


FIG. 2. (Color online) EoS for different sets with a fixed potential depth $U_\Lambda = -28$ MeV.

Now we plot in Fig. 2 the EoS for the four sets presented in Tab. I. We see that the higher the value of $g_{\Lambda,\omega}$, the stiffer the EoS. Unlike Fig. 1 there is no crossing of the curves. This is due to the fact that the main term of the pressure is the vector meson ω and it is proportional to the density n . So, indeed, the curves deviate from each other as the density increases.

Set	M_{max}/M_\odot	$R_{M_{\text{max}}} \text{ (km)}$	$R_{1.4M_\odot} \text{ (km)}$
A	1.45	13.26	13.66
B	1.71	12.68	13.76
C	2.07	12.06	13.74
D	2.31	11.95	13.75

TABLE III. Different sets for Λ -mesons coupling constants with a fixed potential depth $U_\Lambda = -28$ MeV.

To conclude this section we solve the TOV structural equations [31] and plot the mass-radius relation in Fig. 3. Here, and in the rest of this work we use the BPS [32] equation to simulate the neutron star crust. The most massive pulsar yet known is the PSR J0348+0432 [2] with a mass of $2.01 \pm 0.04 M_\odot$. So, for an EoS to be valid, it needs to explain this massive neutron star. Another constraint is the radius of the canonical $1.4M_\odot$ pulsar. According to ref. [8–12] the maximum radius for these stars lie between 12.45 to 13.9 km. We plot the main results for the TOV solutions in Tab. III.

By looking at Fig. 3, we can see that according to ref. [2], only sets C and D are valid as EoS of dense matter. All the radii are very close, between 13.74 km to 13.76 km, except for set A. This is due to the emergence of a new degree of freedom. A new degree of freedom as the Λ hyperon not only reduces the maximum mass, but compresses the neutron star. When the hyperon fraction becomes relevant, there is a “turn to the left” in the mass-radius relation, compressing the subsequent neutron stars, reducing their radii. For a hyperon potential depth of -28 MeV, the threshold of hyperons appears too late for this “turn to the left” affect the canonical $1.4M_\odot$ to values of radii that agree with the ref. [8–12]. But for

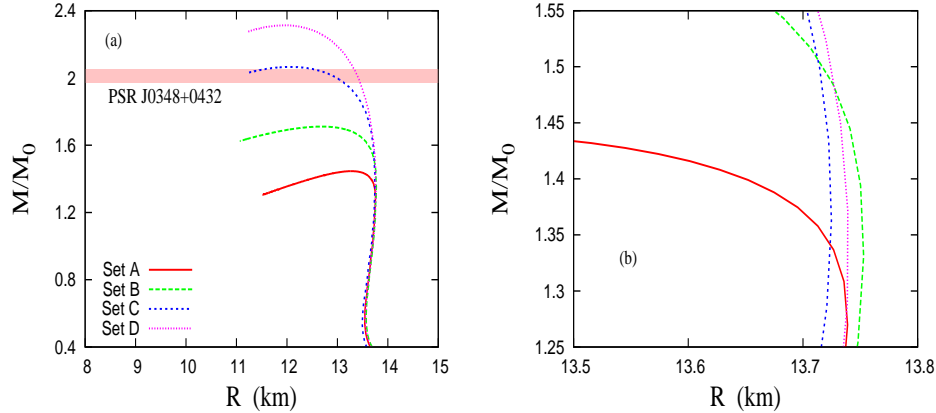


FIG. 3. (Color online) (a) Mass-radius relation obtained via TOV solution, the hatched area comprises the uncertainty about the mass of the PSR J0348+0432. (b) Zoom in the mass around $1.4 M_\odot$.

more massive neutron stars, the large amount of hyperons compresses significantly the star. For instance, if someone wonders about the radius of the $2.01 M_\odot$, the PSR J0348+0432, the answer is 12.91 km, if we assume set C as the best parametrization, or 13.40 km if we choose set D, because the “turn to the left” happens earlier in set C than set D. If we want to compress the canonical $1.4 M_\odot$ neutron star, the Λ threshold needs to take place at earlier densities. To accomplish that, the potential depth needs to be lower.

B. Role of the potential depth

Now we study how a more attractive potential depth affects the neutron stars with hyperons. As mentioned earlier in this work, although the U_Λ is well established around around -28 MeV, the nature of the new degree of freedom is not relevant. Any other particle could be used, just adjusting the values of the coupling constants. Moreover, here we are dealing with highly asymmetric matter, instead of the symmetric matter where the potential was inferred, and the hyperon threshold happens at higher densities than n_0 . Because we want the hyperon onset at lower densities we fix the $\omega - \Lambda$ coupling to be very weak, as in set A of Tab. II. Now we vary only the $\sigma - \Lambda$ coupling. The parametrization utilized are presented in Tab. IV, and we plot the Y_Λ fraction in Fig. 4.

Set	$g_{\Lambda,\omega}/g_{N,\omega}$	$g_{\Lambda,\sigma}/g_{N,\sigma}$	U_Λ (MeV)
E	0.25	0.396	-50
F	0.25	0.476	-80
G	0.25	0.547	-100
H	0.25	0.640	-126

TABLE IV. Different sets for U_Λ with a fixed $\omega - \Lambda$ coupling of $g_{\Lambda,\omega}/g_{N,\omega} = 0.25$.

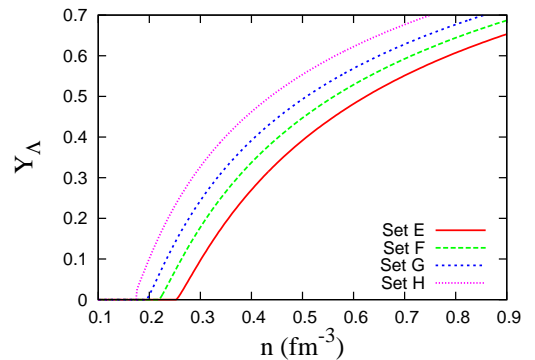


FIG. 4. (Color online) Λ threshold and population for a potential depth U_Λ varying from -50 MeV to -126 MeV.

We can see that the more attractive the U_Λ , the earlier the hyperon threshold. Also, the more attractive the U_Λ , the higher the Y_Λ at high densities. Indeed, the lambda fraction can reach values higher than 0.7 for sets G and H. The Λ potential depth can be as low as -126 MeV. This value was not randomly chosen. As we will see in the next topic, this value is the highest value that is able to predict a massive neutron star with the radius agreeing with ref. [8–12].

Now in Fig. 5 we plot the EoS for different values of U_Λ . Due to the extremely attractive potential, and the great amount of hyperons, we expect very soft EoS. Indeed, as one can see, for sets G and H, the $dp/d\epsilon$ could even be negative. That could indicate a phase transition. These are deeper waters where we will not navigate into [33]. Moreover, since a negative value of $dp/d\epsilon$, produces unstable neutron stars [19], we concentrate this work only in EoS for which $dp/d\epsilon$ is greater than zero. Now we plot the TOV solution for sets E and F in Fig. 6.

Due to the very attractive hyperon potential depth, and once we have a very weak repulsive channel, these soft EoS produces very low maximum mass neutron star.

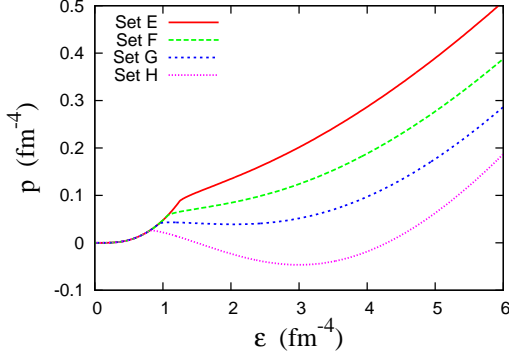


FIG. 5. (Color online) EoS for different sets varying the U_Λ from -50 MeV to -126 MeV.

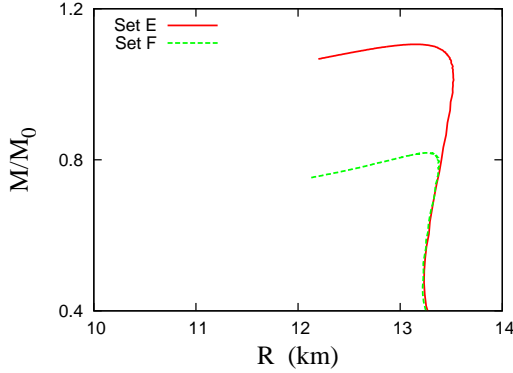


FIG. 6. (Color online) Mass-radius relation for $U_\Lambda = -50$ MeV and $U_\Lambda = -80$ MeV. The “turn to the left” can occur for masses lower than $0.8 M_\odot$.

Also, only for sets E and F it is possible to solve the TOV equations, since it requires $dp/d\varepsilon$ greater than zero. Indeed, all EoS in this section are ruled out, since none of them is able to explain the massive PSR J0348+0432. Nevertheless, the key point in the section is the “turn to the left”. Looking at Fig. 6, we can see that for $U_\Lambda = -80$ MeV, the “turn to the left” occurs for masses below $0.8 M_\odot$. If an even more attractive potential is used, earlier would be this behavior. The star masses are so low due to the very weak repulsive channel. In next section we see how to overcome this issue.

C. Role of the strange vector meson ϕ

We see that the emergence of a new degree of freedom causes a “turn to the left” in the mass-radius relation, compressing the subsequent stars. The earlier the onset of this new particle, the lower the mass that is affected by this “turn to the left”. But we also see that the threshold of a new particle softens the EoS. To stiffen the EoS, we need to increase the repulsive channel. The term responsible to this in eq. (1) is the $\Lambda - \omega$ coupling constant. However, the increase of the $\Lambda - \omega$ channel will affect the

U_Λ potential, and the “turn to the left” will not affect the canonical $1.4 M_\odot$. One way to overcome this difficulty is to add in the Lagrangian a new repulsive channel. We use here the strange vector ϕ meson [26–28]:

$$\mathcal{L}_{YY\phi} = -g_{Y,\phi}\bar{\psi}_Y(\gamma^\mu\phi_\mu)\psi_Y + \frac{1}{2}m_\phi^2\phi_\mu\phi^\mu - \frac{1}{4}\Phi^{\mu\nu}\Phi_{\mu\nu}. \quad (4)$$

Set	$g_{\Lambda,\omega}/g_{N,\omega}$	$g_{\Lambda,\sigma}/g_{N,\sigma}$	$g_{\Lambda,\phi}/g_{N,\omega}$	U_Λ (MeV)
H-I	0.25	0.640	0.650	-126
H-II	0.25	0.640	1.000	-126
H-III	0.25	0.640	1.350	-126
H-IV	0.25	0.640	1.754	-126

TABLE V. Different sets for $g_{\Lambda,\phi}/g_{N,\omega}$ with a fixed $U_\Lambda = -126$ MeV.

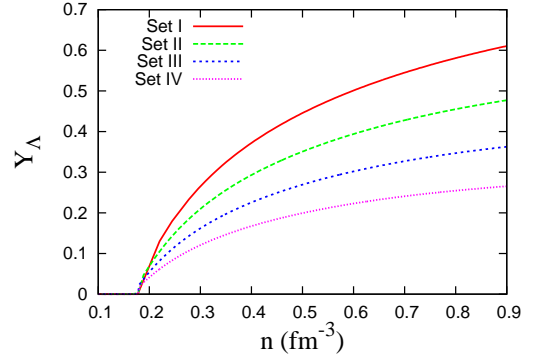


FIG. 7. (Color online) Λ threshold and population for different values of $\Lambda - \phi$ coupling, with a fixed $U_\Lambda = -126$ MeV.

The ϕ field is analogous to the ω field and its expected value is also obtained via MFA [18, 19, 21]. Adding a new mesonic field has two advantages. First, since the ϕ does not couple to the nucleon, it does not affect the properties of the nuclear matter. Second, since the ϕ field is zero below the hyperon threshold density, it does not affect the potential depth, and has little influence on the point of the “turn to the left”. Now we fix the $U_\Lambda = -126$ MeV as in set H. Indeed, all sets in this section are derived from set H of Tab. IV, only varying the $\Lambda - \phi$ coupling constant. So, we numbered the sets from H-I to H-IV. In the figures the H is omitted to not burden the notation. We choose that set because, as we will see, this potential depth is the less attractive potential able to produce a $2.05 M_\odot$ neutron star, with a radius of 12.45 km. The values utilized in this calculation are presented in Tab. V.

Now we plot the Λ fraction in Fig. 7. As we can see, since ϕ field is zero before the hyperon threshold, and the potential depth are the same for all sets, the hyperon onset is the same for all values of $\Lambda - \phi$ coupling, around $0.177 n_0$. This is a relative low value, corresponding to 16% above the nuclear saturation density. Since ϕ is a repulsive channel, the stronger the coupling, the

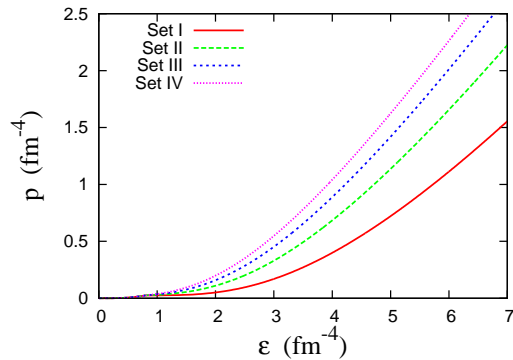


FIG. 8. (Color online) EoS for different values of $\Lambda - \phi$ coupling, with a fixed $U_\Lambda = -126$ MeV. In these cases $dp/d\epsilon$ is always greater than zero.

stronger the hyperon suppression at high densities. Indeed in set H-IV, Y_Λ never surpasses 0.3. Also, the ϕ field contributes in the pressure, stiffening the EoS. Plotting the EoS of Tab. V in Fig. 8, we can see that with the ϕ field, $dp/d\epsilon$ is always positive.

Set	M_{\max}/M_\odot	$R_{M_{\max}}$ (km)	$R_{1.4M_\odot}$ (km)
H-I	1.42	7.91	8.11
H-II	1.72	9.06	10.49
H-III	1.91	9.95	11.70
H-IV	2.05	10.57	12.45

TABLE VI. Main properties of neutron stars with the inclusion of the ϕ meson for $U_\Lambda = -126$ MeV.

Now we plot the mass-radius relation in Fig. 9 with the main properties resumed in Tab. VI. We can see that due to the onset of hyperons at low densities, the “turn to the left” occurs at very low masses. Indeed in set H-I, it happens at mass around $0.5M_\odot$. The higher the $\Lambda - \phi$ coupling, the less pronounced is the compression of the subsequent neutron stars. Also, in set H-I, we see that the canonical $1.4M_\odot$ is only 8.11 km, a very compact neutron star. Nevertheless, its maximum mass of only $1.42M_\odot$ indicates that this EoS must be ruled out.

Increasing the $\Lambda - \phi$ coupling, we also increase the maximum mass. In set H-IV, for a strong coupling, the maximum mass reaches $2.05M_\odot$, the upper limit of the $2.01 \pm 0.04 M_\odot$, PSR J0348+0432 pulsar. But, unlike sets C and D of Fig. 3, now we have a much lower radius for the canonical $1.4M_\odot$. With this modified GM1 model, the radius was around 13.76 km. Now we have a radius of only 12.45 km. In other words, an EoS that is able to explain the massive PSR J0348+0432 [2], and also in agreement with the inferred measures of the pulsar radii [8–12]. We show that the emergence of a new degree of freedom is able to compress the neutron stars and still produce very massive pulsars.

Another good constraint to be assessed is the pressure of symmetric matter for densities up to five times the nuclear saturation density, as inferred in ref. [17] via HIC.

As discussed in ref. [4, 28], the GM1 is in disagreement with this constraint. However, as pointed in ref. [28] this could be due to the fact we are not considering the onset of hyperons in the bulk of nuclear matter. Now we define the symmetric hypernuclear matter as in ref. [28]. Consider a symmetric matter. In this regime, by definition, the density of the protons is equal to the density of neutrons, $n_p = n_n$. Due to this, the ρ field is zero and the chemical potential of these particles are also the same, $\mu_n = \mu_p$. If we compress this matter, the onset of strange particles, as Λ , becomes energetically favorable. Since ref. [17] does not rule out neither hyperons nor even more exotic pictures, such as quark-hadron phase transitions, we assume the possibility of Λ onset in the symmetric matter, imposing:

$$\mu_p = \mu_n = \mu_\Lambda. \quad (5)$$

This choice implies that only symmetric nuclear matter exists until the density is high enough so the creation of strange particles becomes energetically favorable, softening the EoS. The pressure of GM1 symmetric matter and symmetric hypernuclear matter alongside the inferred pressure up to five times nuclear saturation density (hatched area), obtained in ref. [17] are plotted in Fig. 10. Since only set H-IV is able to predict a $2.0M_\odot$ we plot only this set.

The hyperon threshold softens the EoS making experiment results from HIC and theory reach an agreement again. While in beta-equilibrium matter the onset of the new degree of freedom is at densities about 16% above the nuclear saturation density, in symmetric matter this onset happens latter, at densities about 51% above the saturation point. This is due to the fact that the ρ field, that is a repulsive channel is zero, and the nuclear matter has a lower chemical potential compared with the stellar one. Indeed, the nuclear matter is bounded for densities below the saturation density. We see that, the emergence of a new degree of freedom, besides being able to explain the astrophysical observations of a very massive pulsar and the inferred low radius for the canonical mass, reconciles these results with those obtained in laboratory.

D. Role of the strange scalar meson σ^*

Now we give one more step and add a new strange meson, the scalar σ^* . As the vector ϕ meson, the scalar one just couples to the Λ particles, and does not affect any of the properties of nuclear matter presented in Tab. I. Also, the σ^* field is zero in the absence of Λ particles, therefore it would not affect the hyperon threshold. The Lagrangian of σ^* is analogous to the σ and reads:

$$\mathcal{L}_{Y\sigma^*} = g_{Y,\sigma^*}(\bar{\psi}_Y\psi_Y)\sigma^* + \frac{1}{2}\left(\partial^\mu\sigma^*\partial_\mu\sigma^* - m_{\sigma^*}^2\sigma^{*2}\right). \quad (6)$$

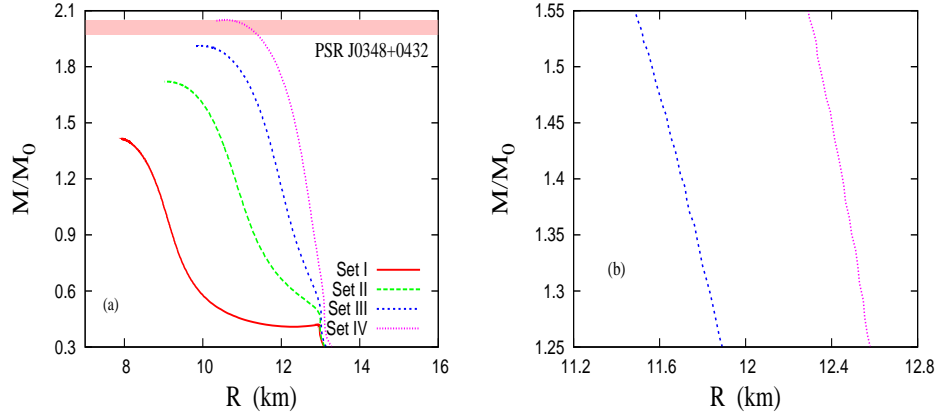


FIG. 9. (Color online) (a) Mass-radius relation obtained via TOV solution with the inclusion of the ϕ meson. The hatched area comprises the uncertainty about the mass of the PSR J0348+0432. (b) Zoom in the mass around $1.4M_\odot$, although sets H-I and H-II are not showed, it is not relevant since its maximum mass is lower than the PSR J0348+0432.

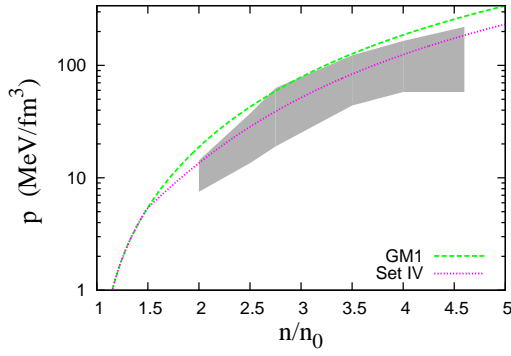


FIG. 10. (Color online) Pressure of symmetric nuclear matter of the GM1 model and the symmetric hypernuclear matter with the onset of a new degree of freedom compared with experimental constraint (hatched area).

Set	$g_{\Lambda,\sigma^*}/g_{N,\sigma}$	$g_{\Lambda,\phi}/g_{N,\omega}$	U_Λ (MeV)
H-V	0.65	1.80	-126
H-VI	1.00	1.88	-126
H-VII	1.50	2.00	-126
H-VIII	2.00	2.02	-126

TABLE VII. Different sets for $g_{\Lambda,\sigma^*}/g_{N,\sigma}$ and $g_{\Lambda,\phi}/g_{N,\omega}$ with a fixed $U_\Lambda = -126$ MeV.

The σ^* is an attractive scalar meson, while the ϕ is a repulsive vector meson. Therefore, the σ^* will dominate at low densities, softening the EoS and increasing the amount of hyperons. At high densities, the ϕ meson dominates, causing a strong suppression of the hyperons and stiffening the EoS. This behavior is analogous to the $\delta - \rho$ competition in the symmetry energy reported in ref. [7]. In Tab. VII we show the values of the coupling constants for the $\Lambda - \sigma^*$ and $\Lambda - \phi$ mesons. All these values have been chosen in such a way that the EoS is

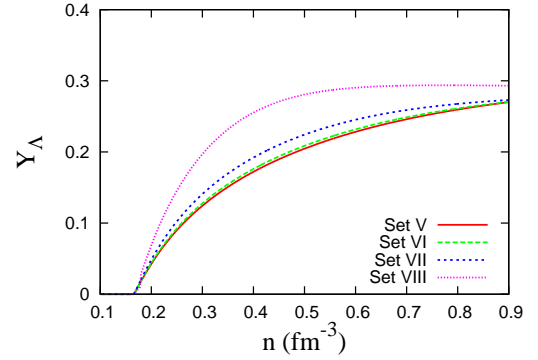


FIG. 11. (Color online) Λ threshold and population for different values of $\Lambda - \sigma^*$ and $\Lambda - \phi$ coupling, with a fixed $U_\Lambda = -126$ MeV.

able to reproduce a $2.05M_\odot$ as a maximum mass. And again, in all cases the set H of Tab. IV is used to fix the hyperon potential depth at -126 MeV.

Now we plot in Fig. 11 the hyperon fraction for the sets of Tab. VII. We see that the σ^* has little influence if the $\Lambda - \sigma^*$ is not high. Sets H-V to H-VII are very similar. For set H-VIII the coupling constant of $\Lambda - \sigma^*$ is two times the $N - \sigma$ one, and the difference is higher. But in all cases, the Y_Λ is low, and again never surpasses 0.3.

The differences in the EoS are even smaller. Since all the EoS are adjusted to reproduce a $2.05M_\odot$ as maximum mass, they are all very similar. Due to this we just plot the set H-V and set H-VIII, that have the weakest and strongest coupling constants. Of course we could increase the repulsive channel and simulate even higher mass neutron stars, however this would imperatively increase the radius of the canonical $1.4M_\odot$. We also plot the results obtained with set C from Tab. II since it predicts similar maximum mass. The results are presented

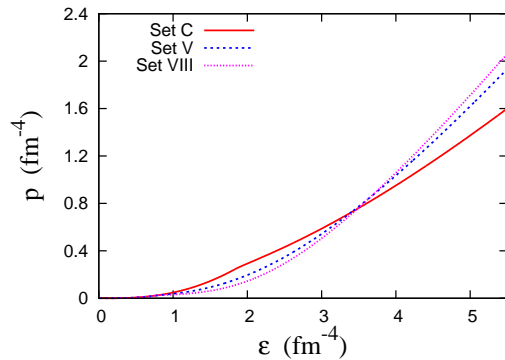


FIG. 12. (Color online) EoS for sets C, H-V and H-VIII.

in Fig. 12. We see that set H-V produces a lower value of $\Lambda - \sigma^*$ and $\Lambda - \phi$ coupling. Due to this, the EoS is less soft at low density and also less stiffer at high density. In set H-III, $\Lambda - \sigma^*$ and $\Lambda - \phi$ coupling are very high. So σ^* meson strongly dominates at low density, softening the EoS, while ϕ stiffens it at high densities. Set C has no hyperons at low densities, so it is stiffer in this regime. Also, due to the absence of the ϕ meson, this set is softer at high densities. Sets H-VI and H-VII are between set H-V and H-VIII. The stronger the interaction with both mesons, the softer it will be at low density and stiffer at higher ones due to the different nature of the mesons (scalar and vector).

Set	M_{\max}/M_{\odot}	$R_{M_{\max}}$ (km)	$R_{1.4M_{\odot}}$ (km)
H-V	2.05	10.54	12.43
H-VI	2.05	10.50	12.38
H-VII	2.05	10.37	12.20
H-VIII	2.05	10.57	11.51

TABLE VIII. Main properties of neutron stars with the inclusion of the σ^* and ϕ mesons for $U_{\Lambda} = -126$ MeV.

Now, let's solve the TOV equations and obtain the mass-radius relation. The results are plotted in Fig 13 and the main relevant properties are resumed in Tab. VIII. The presence of the σ^* softens the EoS at low densities. This behavior causes the “turn to the left” in mass-radius relation to be more pronounced, compressing the subsequent neutron stars and producing a significantly lower value for the radius of the $1.4M_{\odot}$ star. The stronger the $\Lambda - \sigma^*$ coupling, the lower the radius. Indeed this radius can reach 11.51 km for a very strong $\Lambda - \sigma^*$ coupling constant, of two times the $N - \sigma$ one. This limit of two times the $N - \sigma$ one presented in this work is not arbitrary. This is the highest value that produces a neutron star of $2.05M_{\odot}$ with $dp/d\epsilon$ always greater than zero. If we increase the $\Lambda - \sigma^*$ coupling, this condition will be broken. Of course we can increase the $\Lambda - \phi$ coupling constant to avoid a negative value of $dp/d\epsilon$, however it will also increase the maximum mass beyond $2.05M_{\odot}$ and enlarge the radius of the canonical star. With the help of

σ^* meson we are able to simulate neutron stars agreeing with the PSR J0348+0432 [2], and the radii in the range proposed in ref. [8–12]. Comparing the TOV solution with the EoS of Fig. 12 we can also link the radius of canonical stars to a soft EoS at densities not much above the saturation point. This seems a more fundamental relation than linking the radii to the slope. The cause and effect follows: the hyperon onset softens the EoS (at low densities), and this soft EoS produces the “turn to the left” in the mass-radius relation. The strong $\Lambda - \phi$ coupling produces a stiff EoS (at high densities), and this stiff EoS produces very massive neutron stars.

To conclude this section we compare our results for a symmetric hypernuclear matter with the constraint imposed by ref. [17]. Again, due to the fact that the EoS are very similar we plot only set H-V and set H-VIII. Since set H-VI and H-VII have intermediate values for the coupling constants, their results will be always between sets H-V and H-VIII. We see in Fig. 14 that the same effects that happen in β -equilibrium matter are reproduced in symmetric hypernuclear matter. The stronger the $\Lambda - \sigma^*$ coupling, the softer the EoS. But due to the high value of the $\Lambda - \phi$ coupling needed to reproduce very massive pulsars, this EoS will become stiffer at high densities. We conclude that our model with the onset of a new degree of freedom agrees with astrophysical observations and HIC experiments.

IV. FINAL REMARKS

In this work we show how the onset of a new degree of freedom is able to reconcile the recent measurements of very massive pulsars [1, 2] with compact ones [8–12], and also satisfy HIC experimental constraints [17]. Although the true nature of this new degree of freedom is an open puzzle, we show that a particle not much heavier than the nucleon and a new repulsive channel is enough to accomplish this goal. Also, we are able to construct a thermodynamical consistent model with no *ad hoc* inputs.

We start by reviewing the effects of hyperon threshold in dense nuclear matter. The consequent softening of the EoS and reduction of the maximum mass is a well-known theme in the literature [19, 21, 23], but the “turn to be left” when the hyperon fraction becomes relevant seems to have passed unnoticed. We show that for the well-established Λ potential depth of -28 MeV, there is little influence of the hyperon onset in the radii of stars around the canonical mass of $1.4M_{\odot}$.

Next we modify the Λ potential depth allowing it to assume more attractive values. Therefore, the onset of the new degree of freedom appears at lower densities and the “turn to be left” occurs for less massive stars, reaching the canonical mass. Due to the very weak repulsive channel, all resulting neutron stars have very low maximum mass and the corresponding EoS must be ruled out.

To overcome this issue we add a new repulsive chan-

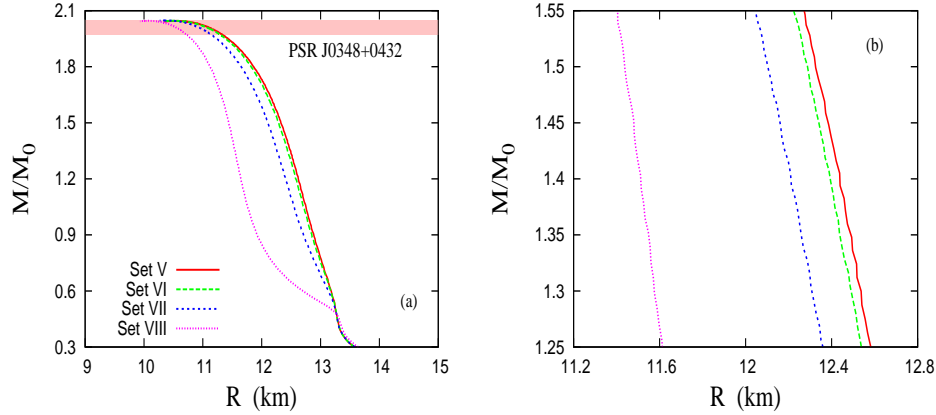


FIG. 13. (Color online) a) Mass-radius relation considering both σ^* and ϕ mesons constrained to a maximum mass of $2.05M_\odot$. b) Zoom in the mass around $1.4M_\odot$. Stronger is the $Y - Y$ interaction, lower are the radii.

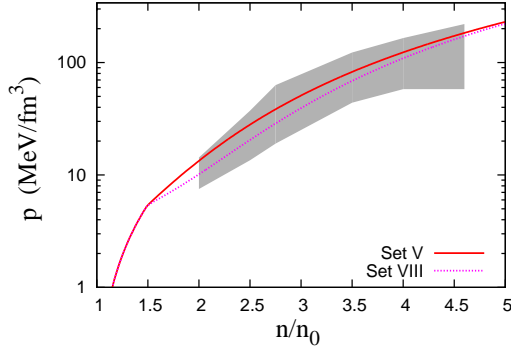


FIG. 14. (Color online) Role of the the σ^* and ϕ mesons in the symmetric hypernuclear matter compared with experimental constraint (hatched area).

nel, through the strange vector ϕ meson. This allows us to stiffen the EoS and increase the maximum mass without change any properties of nuclear matter and with no effect on the hyperon threshold. This also allows us to construct a very realistic EoS, that is able to explain the massive PSR J0348+0432 and the measurements of low radii pulsars. The result is even better when compared with the results of HIC. Now we are able to reconcile astrophysical observation and lab constraints.

In the last part of our work we add a new attractive

channel, the strange scalar σ^* meson. This new attractive field softens the EoS at low densities, making the “turn to be left” more pronounced. This compresses even more the subsequent stars, allowing us to construct an EoS that predicts a maximum mass of $2.05M_\odot$, while the canonical $1.4M_\odot$ has a radius of only 11.51 km. We are also able to link the low radius to a soft EoS at low densities, what seems a more fundamental reason than relating it to the symmetry energy slope. Moreover, the emergence of a new degree of freedom again reconciles this EoS with HIC experiments.

We finish this work by pointing out that the nature of the new degree of freedom needs to be better studied, but it seems that the EoS needs to be soft at low densities to predict very compact neutron stars. However, the radii of canonical neutron stars is not a closed subject. Some studies indicate that their values could be very low, not surpassing 11.1 km [34], close but still below the 11.51 km found in this work. Nevertheless, since it is still an open puzzle, a relatively large *lower* limit of 10.7 km for the canonical neutron star is presented in ref. [35] to account for the causality.

Acknowledgments; DPM acknowledges partial support from CNPq and LLL from CAPES and CE-FET/MG.

-
- [1] P. B. Demorest, et al. *Nature*, **467**, 1081 (2010)
 - [2] J. Antoniadis et al: *Science* **340**, 1233232 (2013)
 - [3] J. Lattimer, M. Prakash, *Phys. Rept.* **621**, (2016) 127
 - [4] R. Cavagnoli, D. P. Menezes, C. Providencia, *Phys. Rev. C* **84**, 065810 (2011)
 - [5] S. Gandolfi, J. Carlson, S. Reddy, *Phys. Rev. C* **85**, 032801(R) (2012)
 - [6] Constança Providência et al, *Eur. Phys. J. A* **50**, 44 (2014)
 - [7] L. L. Lopes, D. P. Menezes, *Braz. J. Phys.* **44**, 774 (2014)
 - [8] K. Hebeler et al, *Phys. Rev. Lett.* **105**, 161102 (2010)
 - [9] J. M. Lattimer, Y. Lim *Astrophys. J.* **771**, 51 (2013)
 - [10] T. Guver, F. Özel, *Astrophys. J. Lett.* **765**, 1 (2013)
 - [11] A. W. Steiner, S. Gandolfi, *Phys. Rev. Lett* **108**, 081102 (2012)
 - [12] A.W. Steiner, J.M. Lattimer, E. Brown, *Astrophys. J.*

- 722**, 33 (2010)
- [13] B. Bertoni, Ann E. Nelson, S. Reddy, Phys. Rev. D **88**, 123505 (2013)
 - [14] I. Goldman et al., Phys. Lett. B **725**, 200 (2013)
 - [15] A. Li, F. Huang, R. Xu, Astrop. Phys. **37**, 70 (2012)
 - [16] S. Mukhopadhyay, et al., arXiv:1612.07093
 - [17] P. Danielewicz et al, Science **298**, 1592 (2002)
 - [18] B. D. Serot, Rep. Prog. Phys. **55**, 1855 (1992)
 - [19] N. K. Glendenning, *Compact Stars*, Springer, New York - Second Edition (2000)
 - [20] J. Boguta, A. R. Bodmer, Nucl. Phys. A **292**, 413 (1977)
 - [21] L. L. Lopes, D. P. Menezes, Braz. J. Phys. **42**, 428 (2012)
 - [22] W. Greiner, L. Neise, H. Stocker, *Thermodynamics and Statistical Mechanics* - (Springer, New York, 1995)
 - [23] N. K. Glendenning, S. A. Moszkowski, Phys. Rev. Lett. **67**, 2414 (1991)
 - [24] D. P. Menezes et al., Phys. Rev. C **89** 055207 (2014)
 - [25] M. G. Paoli, D. P. Menezes, Eur. J. Phys. A **46**, 413 (2010)
 - [26] S. Weissenborn, D. Chatterjee, J. Schaffner-Bielich, Nucl. Phys. A **881**, 62 (2012)
 - [27] S. Weissenborn, D. Chatterjee, J. Schaffner-Bielich, Phys. Rev. C **85**, 065802 (2012)
 - [28] L. L. Lopes, D. P. Menezes, Phys. Rev. C **89**, 025805 (2013)
 - [29] L. L. Lopes, D. P. Menezes, J. Cosm. Astropart. Phys. **08** 02 (2015)
 - [30] P. K. Panda, et al., Phys. Rev. C **85**, 055802 (2012)
 - [31] J. R. Oppenheimer, G. M. Volkoff, Phys. Rev. **55**, 374 (1939)
 - [32] G. Baym, C. Pethick, P. Sutherland, Astrophys. J. **170**, 299 (1971)
 - [33] H. Muller, B. Serot, Phys. Rev. C **52**, 2072 (1995)
 - [34] F. Ozel et al., Astrophys. J. **820**, 28 (2016)
 - [35] W. Chen, J. Piekarewicz Phys. Rev. Lett **115**, 161101 (2015)